

Interaction Effects on Number Fluctuations in a Bose-Einstein Condensate of Light

E.C.I. van der Wurff,^{*} A.-W. de Leeuw, R.A. Duine, and H.T.C. Stoof
*Institute for Theoretical Physics and Center for Extreme Matter and Emergent Phenomena,
 Utrecht University, Leuvenlaan 4, 3584 CE Utrecht, The Netherlands*
 (Dated: March 24, 2014)

We investigate the effect of interactions on condensate-number fluctuations in a Bose-Einstein condensate of photons in a dye-filled optical cavity. For a contact interaction we obtain the equilibrium probability distribution of the number of photons in the condensate variationally. To facilitate comparison with experiment, we also calculate the zero-time delay autocorrelation function $g^{(2)}(0)$ for different strengths of the interaction. We propose that the photon-photon interaction is the result of the interaction of the photons with the dye molecules.

PACS numbers: 67.85.Hj, 42.50.Ar, 42.50.Lc

Introduction.— Fluctuations are ubiquitous in physics: from the primordial quantum fluctuations in the early universe that reveal themselves as fluctuations in the cosmic microwave background, to current fluctuations in every-day conductors. For large voltages, the latter fluctuations give rise to shot noise, that is due to the discrete nature of charge [1]. As a consequence, shot noise can be used to determine the quanta of the electric charge of the current carriers in conducting materials [2]. Indeed, it has been used to characterize the nature of Cooper pairs in superconductors [3] and the fractional charge of the quasiparticles of the quantum Hall effect [4]. For low voltages, the noise in the current is thermal and is called Johnson-Nyquist noise [5, 6]. Contrary to shot noise, thermal noise is always present in electrical circuits, even if no externally applied voltage is present, since it is due to thermal agitation of charge carriers, that leads to fluctuating electromotive forces in the material.

Theoretically, fluctuations in equilibrium are described by the fluctuation-dissipation theorem, as formulated by Nyquist in 1928 and proven decades later [7]. This theorem relates the response of a system to an external perturbation to the fluctuations in the system in the absence of that perturbation. Given a certain fluctuation spectrum we can reconstruct the response of the system. Therefore, this theorem is very powerful, as was fervently argued by the Japanese physicist Kubo [8].

Having stressed the importance of fluctuations in physics and the information they contain, we now zoom in on number fluctuations as our main point of interest. Traditionally, weakly interacting Bose-Einstein condensates were first observed in dilute atomic vapors [9]. For these systems, it is very difficult to measure number fluctuations because number measurements typically are destructive. Therefore, theoretical work has focused more on density-density correlation functions [10, 11]. In recent years, Bose-Einstein condensates of quasiparticles have also been created, such as exciton-polariton condensates [12], magnon condensates [13] and condensates of photons [14, 15]. As these condensates are realized under different circumstances and with different particles

compared to the atomic Bose-Einstein condensates, new experimental possibilities have opened up. For example, large number fluctuations of the order of the total particle number have been observed in a condensate of photons [16].

There have been several theoretical studies focusing on Bose-Einstein condensates of light. One of the studies establishes a theory for a non-interacting condensate of photons based on the hierarchical maximum-entropy principle, predicting sub-Poissonian number statistics under certain circumstances [17]. In another study several characteristics of the system are captured in an effective contact interaction, leading to a Gross-Pitaevskii description for the condensate [18]. Additionally, the molecular degrees of freedom in the system have been described as collective Dicke states rather than individual excitations in Ref. [19]. Finally, some of our own earlier work focuses on the nonequilibrium dynamics of the photon gas [20].

In this Letter we investigate the observed large number fluctuations of the Bose-Einstein condensate of photons. We start by introducing an effective contact interaction into the grand-canonical Hamiltonian of the photon gas and derive an equilibrium probability distribution for the number of photons in the condensate. Subsequently, we investigate these distributions for different condensate fractions and interaction strengths. We also calculate the zero-time delay autocorrelation function $g^{(2)}(0)$ to quantify the number fluctuations and compare this to the experiments, using our interaction strength as a fitting parameter. Finally, we discuss our findings and propose a possible mechanism for the photon-photon interaction.

Interaction effects on number fluctuations.— In the experimental set-up described in Refs. [14–16], photons are confined in a dye-filled cavity. The photons thermalize to the temperature of the dye solution by scattering off the dye molecules. Furthermore, the cavity fixes the longitudinal component of the photon momentum k_z . Therefore, the photons obtain an effective mass m and the photon gas becomes effectively two-dimensional. Since the energy of the photons is larger than the thermal energy,

and photon losses are compensated by external pumping, the average number of photons is constant. Therefore, the photon gas has a nonzero chemical potential, which is a prerequisite for Bose-Einstein condensation. Additionally, Bose-Einstein condensation in a uniform gas in two dimensions can only occur at zero temperature [21]. However, it can occur at a non-zero temperature if the bosons are confined by a harmonic-oscillator potential, which in this experiment is provided by the curvature of the cavity mirrors.

To investigate the number fluctuations, we first calculate the average number of particles $\langle N_0 \rangle$ in the condensate. For this we need the probability distribution $P(N_0)$ for the number of condensed photons. Since the photon system is pumped by an external laser, we treat the system in the grand-canonical ensemble. Thus, the probability distribution is of the form $P(N_0) \propto \exp(-\beta\Omega(N_0))$, with $\Omega(N_0)$ the grand potential of the photon gas. To find the grand potential we use a variational wavefunction approach. In Ref. [14] a rather accurate description of the condensate radius is obtained by approximating the photon self-interaction by a contact interaction. We therefore consider the following energy functional for the macroscopic wavefunction $\phi_0(\mathbf{x})$ of the Bose-Einstein condensate [22]

$$\Omega[\phi_0(\mathbf{x})] = \int d\mathbf{x} \left(\frac{\hbar^2}{2m} |\nabla \phi_0(\mathbf{x})|^2 + V^{\text{ex}}(\mathbf{x}) |\phi_0(\mathbf{x})|^2 - \mu |\phi_0(\mathbf{x})|^2 + \frac{g}{2} |\phi_0(\mathbf{x})|^4 \right), \quad (1)$$

where \mathbf{x} is the two-dimensional position, the first term represents the kinetic energy of the condensate, $V^{\text{ex}}(\mathbf{x}) = m\omega^2|\mathbf{x}|^2/2$ is the harmonic trapping potential, μ is the chemical potential of the photons and g is the coupling constant of the effective pointlike interaction between the photons. We use the Bogoliubov substitution $\phi_0(\mathbf{x}) = \sqrt{N_0}\psi_q(\mathbf{x})$, with the normalized variational wavefunction $\psi_q(\mathbf{x})$, such that $\int d\mathbf{x} |\phi_0(\mathbf{x})|^2 = N_0$. Subsequently, we minimize the energy as a function of the variational parameter q , which describes the width of the condensate. As an ansatz we take the variational wavefunction to be the Gaussian $\psi_q(\mathbf{x}) = (\sqrt{\pi}q)^{-1} \exp(-|\mathbf{x}|^2/2q^2)$. Substituting this into the energy given by Eq. (1) and minimizing with respect to the variational parameter, we obtain

$$q_{\min} = \sqrt[4]{\frac{mN_0g + 2\pi\hbar^2}{2\pi\omega^2m^2}} = q_{\text{ho}} \sqrt[4]{1 + \frac{\tilde{g}N_0}{2\pi}}, \quad (2)$$

where we introduced the dimensionless coupling constant $\tilde{g} := mg/\hbar^2$ and the harmonic oscillator length $q_{\text{ho}} = \sqrt{\hbar/m\omega}$. Note that for a sufficiently small number of condensate particles q_{\min} reduces to q_{ho} . For a large number of condensate particles the Thomas-Fermi ansatz for the wavefunction is in principle more appropriate. However, it is well known from the atomic condensates [23] that even in this case the Gaussian approach is

rather accurate, justifying the further use of the Gaussian ansatz.

We now substitute the minimal value for the variational parameter q into the energy functional, yielding the probability distribution

$$P(N_0) \propto \exp \left(\beta N_0 \left(\mu - \hbar\omega \sqrt{1 + \frac{\tilde{g}N_0}{2\pi}} \right) \right), \quad (3)$$

where the normalization is $\int_0^\infty dN_0 P(N_0) = 1$.

Experimentally, the relevant parameter is the condensate fraction $x := \langle N_0 \rangle / \langle N \rangle$, with N the total number of photons. Thus, to relate our results to the experiments we need a relation between $\langle N_0 \rangle$ and the total number of photons. For temperatures T below the critical temperature for Bose-Einstein condensation, the average number of particles in excited states can in a good approximation be determined from the ideal-gas result. We obtain

$$\langle N_{\text{ex}}(T) \rangle = \int_0^\infty \frac{g(\epsilon) d\epsilon}{\exp(\epsilon/k_B T) - 1} = \frac{1}{3} \left(\frac{\pi k_B T}{\hbar\omega} \right)^2, \quad (4)$$

where we used the density of states $g(\epsilon) = 2\epsilon/(\hbar\omega)^2$ for the two-dimensional harmonic trapping potential [21]. The factor of two comes from the two possible polarizations of the photons. The critical temperature T_c is defined by $\langle N \rangle = \langle N_{\text{ex}}(T_c) \rangle$. With this criterion, we find

$$\langle N_0 \rangle = \frac{x}{3(1-x)} \left(\frac{\pi k_B T}{\hbar\omega} \right)^2. \quad (5)$$

As expected, $N_0 \geq 0$ since the fraction x obeys $0 \leq x \leq 1$.

Results.— Given an interaction strength \tilde{g} , we use the normalized probability distribution in Eq. (3) to calculate the chemical potential as a function of $\langle N_0 \rangle$, i.e. $\mu = \mu(\langle N_0 \rangle)$. Given a condensate fraction x , we then use Eq. (5) to calculate $\langle N_0 \rangle$ and the corresponding μ . Finally, we use the obtained chemical potential to plot the probability distribution at fixed x and \tilde{g} . Typical plots of the probability distribution for different condensate fractions are displayed in Fig. 1. Clearly, we have Poissonian behavior for small condensate fractions and Gaussian behavior for larger condensate fractions. Physically, this shows that the effect of repulsive interactions is to reduce number fluctuations, as the interactions give fluctuations an energy penalty. Increasing the interaction strength yields Gaussian behavior for even smaller condensate fractions. These Gaussians are also more strongly peaked around $\langle N_0 \rangle$ for higher interaction strengths, as is to be expected: stronger interactions between the photons cause the fluctuations to be more suppressed.

Next, we obtain also the second moment $\langle N_0^2 \rangle$ from the probability distribution $P(N_0)$. This gives us all the ingredients needed to quantify the number fluctuations

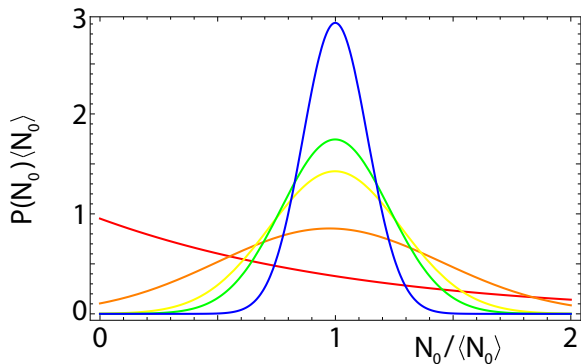


FIG. 1. (color online). Typical plot of the probability distribution for a fixed interaction strength $\tilde{g} = 5 \cdot 10^{-6}$ and different fixed condensate fractions, with $x_{\text{red}} = 0.04$, $x_{\text{orange}} = 0.28$, $x_{\text{yellow}} = 0.40$, $x_{\text{green}} = 0.45$ and $x_{\text{blue}} = 0.58$.

of the condensate in terms of the zero-time delay autocorrelation function $g^{(2)}(0)$, which is defined as

$$g^{(2)}(0) := \frac{\langle N_0^2 \rangle}{\langle N_0 \rangle^2}. \quad (6)$$

A plot of this quantity against the condensate fraction is displayed in Fig. 2 for different interaction strengths \tilde{g} . We note that photon bunching takes place for all interactions at small condensate fractions. For larger condensate fractions $g^{(2)}(0) \rightarrow 1$. The interpretation is as follows. Suppose we fix the condensate fraction x . At small interactions the quartic term in the energy in Eq. (1) is small and the minima of the energy are small and broad, yielding large number fluctuations. If we increase the interaction, the minima become deeper and more narrow, effectively reducing the fluctuations. The same reasoning holds for a fixed interaction strength and increasing condensate fractions, as we can also see in Fig. 1.

Discussion.— In Fig. 2 we fit our theoretical curves to the experimental results obtained by Klaers *et al.*, where it must be noted that the experimental results for small condensate fractions are unreliable due to systematic measurement errors, as is discussed in Ref. [16]. Indeed, we must have $g^{(2)}(0) \rightarrow 2$ for $x \rightarrow 0$. The interaction strength is obtained, resulting into values ranging between 10^{-7} and 10^{-4} for the dimensionless parameter \tilde{g} . Unfortunately, only one independent measurement of the interaction has been performed up to now. This was achieved by measuring the diameter of the condensate for different condensate fractions and fitting this to a numerical solution of the Gross-Pitaevskii equation, yielding a value of $\tilde{g} = (7 \pm 3) \cdot 10^{-4}$ [14] that is close to the value $\tilde{g}_{\text{purple}} = 2 \cdot 10^{-4}$ for the purple curve in Fig. 2. However, it must be noted that the fits are sensitive to changes in the trapping frequency ω and temperature T . We used $\omega = 8\pi \cdot 10^{10}$ Hz and $T = 300$ K, but small changes in these parameters can change the value of \tilde{g} significantly.

The experiments leading to the data points in Fig. 2

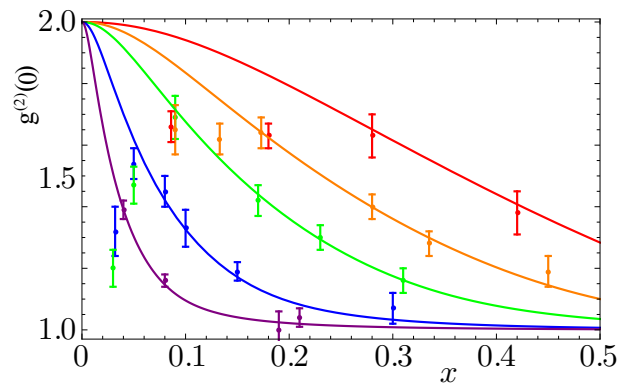


FIG. 2. (color online). Plot of the zero-time delay autocorrelation function $g^{(2)}(0)$ against the condensate fraction x for $\omega = 8\pi \cdot 10^{10}$ Hz and $T = 300$ K. The different curves correspond to different interaction strengths: $\tilde{g}_{\text{red}} = 5 \cdot 10^{-7}$, $\tilde{g}_{\text{orange}} = 2 \cdot 10^{-6}$, $\tilde{g}_{\text{green}} = 5 \cdot 10^{-6}$, $\tilde{g}_{\text{blue}} = 3 \cdot 10^{-5}$, $\tilde{g}_{\text{purple}} = 2 \cdot 10^{-4}$. The curves are fit to the included experimental points from Klaers *et al.* [16].

were performed for two dyes at different molecule densities n_{mol} and detunings δ . The latter is roughly the difference between the cavity frequency and a dye specific frequency related to the absorption threshold of the dye molecules. To be able to explain the experiments as an effect due to interactions, we must have an interaction which is a function of both n_{mol} and the detuning δ . In fact, we can conclude from the experimental data in Fig. 2 that the interaction behaves counter-intuitively: it decreases both for an increasing molecule density and for a decreasing detuning.

Thus, the question that remains to be answered is which mechanism causes the photon-photon interaction, with the correct behavior as a function of n_{mol} and δ . A possible mechanism is displayed in the form of a Feynman diagram in Fig. 3. This box diagram describes mediation of two-photon scattering via dye molecules and results in a non-zero value of \tilde{g} .

In our earlier work in Ref. [20], we adopted a simplified description of the complex rovibrational structure of the dye molecules by describing them as an effective two-level system and by giving the molecules an effective mass. Following this treatment, it turns out that the above diagram contains a divergency of the form $(\mu - \delta)^{-1}$. This is similar to the Feshbach resonances known from cold-atom physics [22, 24]. To get around this non-physical divergence, we introduce a finite decay rate Γ for the excited molecules, with which we are still able to reproduce the correct self-energy of the photons. We show in the supplemental material that

$$\tilde{g}(\mu) = \frac{mg_{\text{mol}}^4 \beta n_{\text{mol}}}{\hbar^4 \Gamma^2 D_0} f(\mu - \delta), \quad (7)$$

where g_{mol} is the coupling strength of the photons to the molecules, $D_0 = 7\pi/k_z$ is the length scale associ-

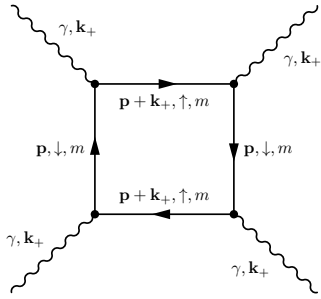


FIG. 3. Feynman diagram for a fourth-order photon-photon interaction. The photons γ are considered to be part of the condensate and are thus at zero frequency and momentum $\mathbf{k}_+ = (0, 0, k_z)$, as their z-component momentum is fixed and $k_x = k_y = 0$ for the ground state of the homogeneous photon gas. The molecule forms a closed loop of ground (\downarrow) and excited (\uparrow) states, with momentum \mathbf{p} and Matsubara frequency ω_m .

ated to the fixed longitudinal momentum of the photons and $f(\mu - \delta)$ is a smooth dimensionless function peaked around zero.

Similar to the procedure followed in Ref. [20] we calculate the self-energy of the photons and fit it to the experimental absorption spectrum of the used dye to obtain g_{mol} , Γ and δ . Due to the introduction of the finite lifetime Γ , \tilde{g} is no longer divergent, but simply peaked around the detuning δ . Subsequently, we have to solve for \tilde{g} self-consistently with the Gross-Pitaevskii equation. Considering the center of the trap, i.e., $V^{\text{ex}} = 0$, this amounts to solving $\tilde{g}(\mu) = (m/\hbar^2 n_{\text{ph}})\mu$ for μ , with n_{ph} the photon density. Graphically, this means that we need to find the intersection of $\tilde{g}(\mu)$ and $(m/\hbar^2 n_{\text{ph}})\mu$.

If the magnitude of \tilde{g} and the slope $m/\hbar^2 n_{\text{ph}}$ are such that the intersection occurs on the right side of the peak in \tilde{g} , increasing the molecule density (and thus proportionally \tilde{g}) means that the point of intersection moves to the right. This implies that the strength of the interaction decreases. A graphical representation is given in Fig. 4. This is exactly the counter-intuitive behavior we are looking for. In order to relate the interaction strength \tilde{g} to the detuning, we note that \tilde{g} only depends on $\mu - \delta$. Therefore, by changing δ we shift the position of the maximum of \tilde{g} . Thus, if we alter δ such that \tilde{g} moves to the left, the interaction strength decreases. In conclusion, this box diagram yields a possible mechanism for the counter-intuitive behavior of the interaction that we found by comparing our theory for photon condensate-number fluctuations to available experiments [16].

Our approximations do not allow for reliable quantitative predictions of the strength of the interaction \tilde{g} . Indeed, due to the large amount of only approximately known experimental parameters in Eq. (7) and the fit to the experimental absorption cross section to obtain the coupling g_{mol} , the magnitude of \tilde{g} is rather uncertain. Therefore, it would be useful to perform systematic mea-

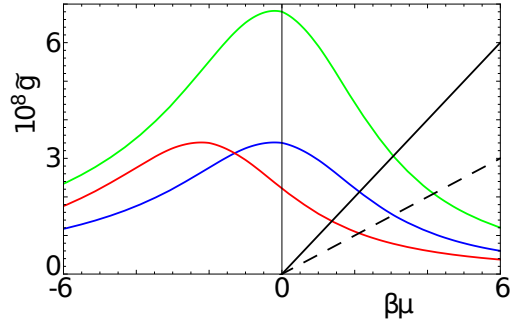


FIG. 4. (color online). The dimensionless interaction parameter \tilde{g} as a function of the chemical potential $\beta\mu$. We used $T = 300$ K, $\beta\hbar\Gamma = 2.9$, $D_0 = 1.46$ μm , $g = 4.1 \cdot 10^{-33}$ $\text{J}\cdot\text{m}^{3/2}$ (chosen such that we reproduce the photon self-energy) and $m = 6.7 \cdot 10^{-36}$ kg. The blue curve is for $n_{\text{mol}} = 9 \cdot 10^{23}$ m^{-3} and $\beta\delta = 4.9$. The green curve has twice the molecule density and the red curve has unchanged n_{mol} but $\beta\delta = 2.9$. As an illustration, the black curve has slope 10^{-8} and the dashed black curve $0.5 \cdot 10^{-8}$. The intersection of the black and blue curve yields the correct μ for the parameters of the blue curve. Doubling n_{mol} we can either find the intersection of the green curve and the black line, or the intersection of the blue curve with the dashed curve, which has half the slope. In the latter case we explicitly see \tilde{g} decreasing.

surements of \tilde{g} for different detunings and molecule concentrations, as is also proposed in Ref. [18]. With this information, we would be able to directly compare our theoretical predictions for the number fluctuations with experimental results, regardless of the mechanism of interactions.

In conclusion, we have determined the influence of photon self-interactions on condensate-number fluctuations in a partially condensed photon gas. By comparing this theory with available experimental results, we found that the interactions should decrease with increasing dye density and decreasing detuning. As a possible mechanism for this counter-intuitive behavior, we propose a contact photon-photon interaction mediated by the dye molecules. Systematic measurements of the interaction strength are necessary to understand the true nature of the interaction. If the interaction is indeed a contact interaction at long wavelengths, then this would imply that the photon condensate is also a superfluid.

It is a pleasure to thank Dries van Oosten, Jan Klaers and Martin Weitz for useful discussions and the latter two also for providing experimental data. This work is supported by the Stichting voor Fundamenteel Onderzoek der Materie (FOM) and is part of the D-ITP consortium, a program of the Netherlands Organisation for Scientific Research (NWO) that is funded by the Dutch Ministry of Education, Culture and Science (OCW).

* e.c.i.vanderwurff@students.uu.nl

- [1] C. Beenakker and C. Schönenberger, *Physics Today* **56**, 37 (2003).
- [2] W. Schottky, *Ann. Phys.* **57**, 541 (1918).
- [3] F. Lefloch, C. Hoffmann, M. Sanquer and D. Quirion, *Phys. Rev. Lett.* **90**, 067002 (2003).
- [4] R. de-Picciotto et al., *Nature* **389**, 162 (1997).
- [5] H. Nyquist, *Phys. Rev.* **32**, 110 (1928).
- [6] J. Johnson, *Phys. Rev.* **32**, 97 (1928).
- [7] H.B. Callen and T.A. Welton *Phys. Rev.* **83**, 34 (1951).
- [8] R. Kubo, *Rep. Prog. Phys.* **29**, 255 (1966).
- [9] M. H. Anderson, J.R. Ensher, M.R. Matthews, C.E. Wieman, E. A. Cornell, *Science* **269**, 5221 (1995).
- [10] E. Altman, E. Demler and M. Lukin, *Phys. Rev. A* **70**, 013603 (2004).
- [11] N. Cherroret and S.E. Skipetrov, *Phys. Rev. Lett.* **101**, 190406 (2008).
- [12] J. Kasprzak et al., *Nature* **443**, 409 (2006).
- [13] S. O. Demokritov et al., *Nature* **443**, 430 (2006).
- [14] J. Klaers, J. Schmitt, F. Vewinger and M. Weitz, *Nature* **468**, 545 (2010).
- [15] J. Klaers, J. Schmitt, T. Damm, F. Vewinger and M. Weitz, *Appl. Phys. B* **105**, 17 (2011).
- [16] J. Schmitt, T. Damm, D. Dung, F. Vewinger, J. Klaers and M. Weitz, *Phys. Rev. Lett.* **112**, 030401 (2014).
- [17] D. N. Sob'yanin, *Phys. Rev. E* **88**, 022132 (2013).
- [18] R. A. Nyman, M. H. Szymanska, arXiv:1308.3588 [quant-ph] (2013).
- [19] E. Sela, A. Rosch and V. Fleurov, arXiv:1309.7575 [cond-mat.quant-gas] (2013).
- [20] A.-W. de Leeuw, H.T.C. Stoof and R.A. Duine, *Phys. Rev. A* **88**, 033829 (2013).
- [21] H. Smith and C.J. Pethick, *Bose-Einstein Condensation in Dilute Gases*, Cambridge University Press, Cambridge, 2nd Edition (2008).
- [22] H.T.C. Stoof, K.B. Gubbels and D.B.M. Dickerscheid, *Ultracold Quantum Fields*, Springer (2009).
- [23] G. Baym and C. J. Pethick, *Phys. Rev. Lett.* **76**, 6 (1996).
- [24] C. Chin, R. Grimm, P. Julienne and E. Tiesinga, *Rev. Mod. Phys.* **82**, 1225 (2010).

Supplemental Material for “Interaction Effects on Number Fluctuations in a Bose-Einstein Condensate of Light”

E.C.I. van der Wurff,* A.-W. de Leeuw, R. A. Duine, and H. T. C. Stoof
*Institute for Theoretical Physics and Center for Extreme Matter and Emergent Phenomena,
 Utrecht University, Leuvenlaan 4, 3584 CE Utrecht, The Netherlands*
 (Dated: March 21, 2014)

This supplemental material provides a more detailed derivation of the box diagram for the photon-photon interaction. We start by considering an action that incorporates the coupling between the photons and the dye molecules. By integrating out the molecular fields, we arrive at an effective action for the photons, including a self-energy and a four-point interaction vertex for the photons. Via an explicit calculation of the self-energy of the photons, we are able to fit the coupling strength between atoms and molecules, the lifetime of the excited state and the detuning to the experimentally known absorption cross section. Hereafter, we give an explicit expression for the box diagram and we obtain numerical values for the interaction strength by using these particular values of the parameters.

I. EFFECTIVE ACTION

In order to describe the system of Bose-Einstein condensed photons, we consider the following Euclidean action [1]

$$\begin{aligned}
 S &= \sum_{\mathbf{k},n} a_{\mathbf{k},n}^* (-i\hbar\omega_n + \epsilon_\gamma(\mathbf{k}) - \mu) a_{\mathbf{k},n} + \sum_{\mathbf{p},\rho,n} b_{\mathbf{p},\rho,n}^* (-i\hbar\omega_n + \epsilon(\mathbf{p}) - \mu_\rho + K_\rho) b_{\mathbf{p},\rho,n} \\
 &+ \frac{g_{\text{mol}}}{\sqrt{\hbar\beta V}} \sum_{\mathbf{k},\mathbf{p},n,n'} \left(a_{\mathbf{k},n} b_{\mathbf{p},\downarrow,n'} b_{\mathbf{p}+\mathbf{k},\uparrow,n+n'}^* + a_{\mathbf{k},n}^* b_{\mathbf{p}+\mathbf{k},\uparrow,n+n'} b_{\mathbf{p},\downarrow,n'}^* \right) \\
 &:= S_\gamma + S_0 + S_{\text{int}},
 \end{aligned} \tag{1}$$

where V is the three-dimensional volume of the system, $\beta := 1/k_B T$ is the inverse thermal energy, g_{mol} is the coupling constant between the atoms and the molecules, $\epsilon(\mathbf{p}) = \hbar^2 |\mathbf{p}|^2 / 2M$ is the dispersion relation for the molecules with mass M and $\epsilon_\gamma(\mathbf{k}) = \hbar c_{\text{med}} \sqrt{k_x^2 + k_y^2 + k_z^2}$ the dispersion relation for the photons, in which k_z is the fixed longitudinal momentum and c_{med} the speed of light in the medium. In the action, we introduced the photon field amplitude $a_{\mathbf{k},n}$ and molecule field amplitude $b_{\mathbf{p},\rho,n}$. The photon fields are bosonic and we model the molecules as fermions, although this is not important since in the end we always consider the classical limit for the dye molecules. Additionally, we model the molecules as a two-level system consisting of an excited state (\uparrow) and ground state (\downarrow). Furthermore, the associated energies of the states are given by $K_\uparrow = \Delta$ and $K_\downarrow = 0$. We use the convention that a sum over \mathbf{p} is three-dimensional, whereas a sum over \mathbf{k} is a two-dimensional sum over a three-dimensional vector with a fixed z -component. Finally, the last two terms describe the absorption and emission of a photon.

From the action we read off the propagators of the non-interacting theory in Fourier space

$$\begin{cases} G_\gamma(\mathbf{k}, i\omega_n) = -\hbar(-i\hbar\omega_n + \epsilon_\gamma(\mathbf{k}) - \mu)^{-1}, \\ G_\rho(\mathbf{k}, i\omega_n) = -\hbar(-i\hbar\omega_n + \epsilon(\mathbf{k}) - \mu_\rho + K_\rho)^{-1}, \end{cases} \tag{2}$$

where ω_n denote the appropriate Matsubara frequencies. By using the action, we write down the partition function Z of the theory as a path integral over the photonic and molecular fields. Subsequently, we perform perturbation theory in the interaction parameter g_{mol} to integrate out the molecules [2], i.e.,

$$\begin{aligned}
 Z &= \int \mathcal{D}[a^*] \mathcal{D}[a] \mathcal{D}[b_\downarrow^*] \mathcal{D}[b_\downarrow] \mathcal{D}[b_\uparrow^*] \mathcal{D}[b_\uparrow] \exp \left(-\frac{1}{\hbar} (S_\gamma + S_0 + S_{\text{int}}) \right) \\
 &= \int \mathcal{D}[a^*] \mathcal{D}[a] \exp \left(-\frac{1}{\hbar} S_\gamma \right) \left(1 + \frac{1}{2\hbar^2} \langle S_{\text{int}}^2 \rangle_0 + \frac{1}{24\hbar^4} \langle S_{\text{int}}^4 \rangle_0 + \mathcal{O}(g_{\text{mol}}^6) \right),
 \end{aligned}$$

*e.c.i.vanderwurff@students.uu.nl

where we used the fact that $\langle S_{\text{int}}^m \rangle_0 = 0$ if m is odd. By using Wick's theorem, we find for the term at order g_{mol}^2

$$\langle S_{\text{int}}^2 \rangle = -\frac{2g_{\text{mol}}^2}{\hbar\beta V} \sum_{\mathbf{k}, \mathbf{p}, n, n'} a_{\mathbf{k}, n}^* a_{\mathbf{k}, n} G_{\uparrow}(\mathbf{p} + \mathbf{k}, i(\omega_n + \omega_{n'})) G_{\downarrow}(\mathbf{p}, i\omega_{n'}). \quad (3)$$

This term can be interpreted as a self-energy for the photons. A diagrammatic representation of this self-energy is depicted in Fig. 1. We do a similar computation for the term at order g_{mol}^4 . Expanding out the interaction term yields

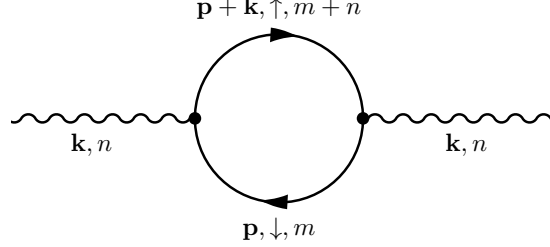


FIG. 1. The Feynman diagram corresponding to Eq. (3). This diagram represents the self-energy of the photons.

sixteen terms, of which ten do not contain the appropriate combination of fields to yield a non-zero result when we Wick contract them. The remaining six terms turn out to be identical, yielding

$$\begin{aligned} \langle S_{\text{int}}^4 \rangle_0 &= \frac{12g_{\text{mol}}^4}{(\hbar\beta V)^2} \sum_{\mathbf{p}, \mathbf{k}, n, n'} \sum_{\mathbf{k}', \mathbf{k}'', m, n''} a_{\mathbf{k}, n}^* a_{\mathbf{k}', n'} a_{\mathbf{k}'', n''}^* a_{\mathbf{k} - \mathbf{k}' + \mathbf{k}'', n - n' + n''} G_{\uparrow}(\mathbf{p} + \mathbf{k}, i(\omega_m + \omega_{n'})) G_{\downarrow}(\mathbf{p}, i\omega_m) \\ &\quad \times G_{\uparrow}(\mathbf{p} + \mathbf{k}', i(\omega_m + \omega_{n'})) G_{\downarrow}(\mathbf{p} + \mathbf{k}' - \mathbf{k}'', i(\omega_m + \omega_{n'} - \omega_{n''})) \\ &\quad - \frac{12g_{\text{mol}}^4}{(\hbar\beta V)^2} \left(\sum_{\mathbf{p}, \mathbf{k}, n, n'} a_{\mathbf{k}, n}^* a_{\mathbf{k}, n} G_{\uparrow}(\mathbf{p} + \mathbf{k}, i(\omega_n + \omega_{n'})) G_{\downarrow}(\mathbf{p}, i\omega_n) \right)^2. \end{aligned} \quad (4)$$

The first term is diagrammatically displayed as a box diagram in Fig. 2. The second term can be represented by a

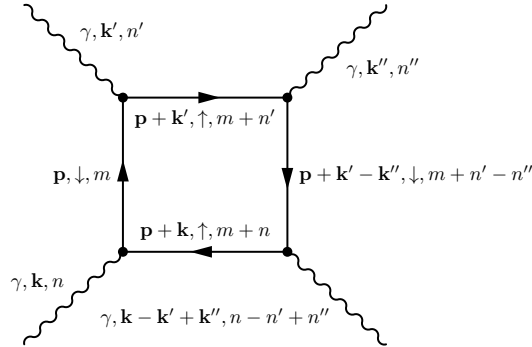


FIG. 2. The Feynman diagram corresponding to the first term in Eq. (4).

disconnected diagram: it is simply one half times the square of the self-energy diagram. Due to the linked-cluster theorem all disconnected diagrams can be summed into an exponent and therefore ignored when calculating the effective action for the photons. Hence, the sum of the self-energy and the box diagram gives us the desired effective action

$$\begin{aligned} S^{\text{eff}} &= \sum_{\mathbf{k}, n} a_{\mathbf{k}, n}^* (-i\hbar\omega_n + \epsilon_{\gamma}(\mathbf{k}) - \mu + \hbar\Sigma(\mathbf{k}, i\omega_n)) a_{\mathbf{k}, n} \\ &\quad + \frac{1}{2\hbar\beta V} \sum_{\mathbf{k}, \mathbf{k}', \mathbf{k}''} \sum_{n, n', n''} \Gamma^{(4)}(\mathbf{k}, \mathbf{k}', \mathbf{k}'', i\omega_n, i\omega_{n'}, i\omega_{n''}) a_{\mathbf{k}, n}^* a_{\mathbf{k}', n'} a_{\mathbf{k}'', n''}^* a_{\mathbf{k} - \mathbf{k}' + \mathbf{k}'', n - n' + n''}, \end{aligned}$$

where we defined the self-energy as

$$\hbar\Sigma(\mathbf{k}, i\omega_n) := \frac{g_{\text{mol}}^2}{\hbar^2\beta V} \sum_{\mathbf{p}, m} G_{\downarrow}(\mathbf{p}, i\omega_m) G_{\uparrow}(\mathbf{p} + \mathbf{k}, i(\omega_n + \omega_m)), \quad (5)$$

and the photon-photon interaction vertex is given by

$$\begin{aligned} \Gamma^{(4)}(\mathbf{k}, \mathbf{k}', \mathbf{k}'', i\omega_n, i\omega_{n'}, i\omega_{n''}) := & -\frac{g_{\text{mol}}^4}{\hbar^4\beta V} \sum_{\mathbf{p}, m} G_{\uparrow}(\mathbf{p} + \mathbf{k}, i(\omega_m + \omega_n)) G_{\downarrow}(\mathbf{p}, i\omega_m) \\ & \times G_{\uparrow}(\mathbf{p} + \mathbf{k}', i(\omega_m + \omega_{n'})) G_{\downarrow}(\mathbf{p} + \mathbf{k}' - \mathbf{k}'', i(\omega_m + \omega_{n'} - \omega_{n''})). \end{aligned} \quad (6)$$

II. SELF-ENERGY

We are interested in calculating the self-energy given by Eq. (5). However, to circumvent divergencies when calculating the photon-photon interaction we first introduce a finite lifetime for the excited molecular state. To do this we recall that the spectral function $\rho(\mathbf{k}, \omega)$ is defined as

$$\rho(\mathbf{k}, \omega) := -\frac{1}{\pi\hbar} \text{Im} \left[G^{(+)}(\mathbf{k}, \omega) \right], \quad (7)$$

where the retarded Green's function follows from a Wick rotation of the Green's function: $G^{(+)}(\mathbf{k}, \omega) = G(\mathbf{k}, i\omega_n \rightarrow \omega + i0)$. Given a spectral function, we calculate the corresponding Green's function by using the following relation

$$G_{\uparrow}(\mathbf{k}, i\omega_n) = \hbar \int_{-\infty}^{\infty} d\omega \frac{\rho_{\uparrow}(\mathbf{k}, \omega)}{i\omega_n - \omega}. \quad (8)$$

For a free theory the spectral function is just a delta function centered around the single-particle energy. We give the excited molecule a finite lifetime by broadening the spectral function to a Gaussian profile, i.e.,

$$\rho_{\uparrow}(\mathbf{k}, \omega) = \frac{1}{\sqrt{2\pi}\hbar\Gamma} \exp \left(-\frac{(\hbar\omega - \epsilon(\mathbf{k}) - \Delta + \mu_{\uparrow})^2}{2(\hbar\Gamma)^2} \right), \quad (9)$$

such that the spectral function satisfies the frequency sum rule $\int_{-\infty}^{\infty} d\hbar\omega \rho_{\uparrow}(\mathbf{k}, \omega) = 1$. Note that this spectral function is still centered around the single-particle energy of the excited molecule and that we have

$$\lim_{\Gamma \rightarrow 0} \rho_{\uparrow}(\mathbf{k}, \omega) = \delta(\hbar\omega - \epsilon(\mathbf{k}) - \Delta + \mu_{\uparrow}). \quad (10)$$

We consider the molecules in the classical limit. Thus, by using the Maxwell-Boltzmann distribution $N_{\text{MB}}(x) := \exp(-\beta x)$, the molecule density in the excited state n_{\uparrow} is equal to

$$\begin{aligned} n_{\uparrow} &= \frac{1}{V} \int_{-\infty}^{\infty} d\hbar\omega \sum_{\mathbf{k}} \rho_{\uparrow}(\mathbf{k}, \omega) N_{\text{MB}}(\hbar\omega) \\ &= \frac{1}{\Lambda^3} \exp \left(\beta\mu_{\uparrow} - \beta\Delta + \frac{1}{2}(\beta\hbar\Gamma)^2 \right), \end{aligned} \quad (11)$$

where the thermal de Broglie wavelength Λ is defined as $\Lambda := \sqrt{2\pi\beta\hbar^2/M}$. Note that in the ground state the molecules still have an infinite lifetime and therefore the density of molecules in the ground state is given by $n_{\downarrow} = \Lambda^{-3} \exp(\beta\mu_{\downarrow})$. We express the chemical potential of the ground state in terms of $\Delta\mu := \mu_{\uparrow} - \mu_{\downarrow}$ and $n_{\text{mol}} := n_{\downarrow} + n_{\uparrow}$ as

$$\exp(\beta\mu_{\downarrow}) = \frac{n_{\text{mol}}\Lambda^3}{1 + \exp(\beta(\Delta\mu - \Delta) + (\hbar\beta\Gamma)^2/2)}, \quad (12)$$

which is a relation we will use later on. We now explicitly calculate the self-energy by starting from the definition provided in Eq. (5) and invoking Eqs. (8) and (9)

$$\begin{aligned}\hbar\Sigma(\mathbf{k}, i\omega_n) &= \frac{g_{\text{mol}}^2}{\hbar^2\beta V} \sum_{\mathbf{p}, m} G_{\downarrow}(\mathbf{p}, i\omega_m) G_{\uparrow}(\mathbf{p} + \mathbf{k}, i(\omega_m + \omega_n)) \\ &= \frac{g_{\text{mol}}^2}{\hbar\beta V} \sum_{\mathbf{p}, m} \int_{-\infty}^{\infty} d\hbar\omega' \left(\frac{\rho_{\uparrow}(\mathbf{p} + \mathbf{k}, \omega')}{i\hbar(\omega_n + \omega_m) - \hbar\omega'} \right) \left(\frac{-\hbar}{-i\hbar\omega_m + \epsilon(\mathbf{p}) - \mu_{\downarrow}} \right) \\ &= \frac{g_{\text{mol}}^2}{V} \sum_{\mathbf{p}} \int_{-\infty}^{\infty} d\hbar\omega' \left(\frac{\rho_{\uparrow}(\mathbf{p} + \mathbf{k}, \omega')}{-i\hbar\omega_n + \hbar\omega' - \epsilon(\mathbf{p}) + \mu_{\downarrow}} \right) \left(N_{\text{FD}}(\hbar\omega') - N_{\text{FD}}(\epsilon(\mathbf{p}) - \mu_{\downarrow}) \right),\end{aligned}$$

where we performed the Matsubara summation and introduced the Fermi-Dirac distribution, which is defined as $N_{\text{FD}}(x) := (\exp(\beta x) + 1)^{-1}$. Since we are considering a bath of molecules at room temperature, we are allowed to take the limit $N_{\text{FD}}(x) \rightarrow N_{\text{MB}}(x) := \exp(-\beta x)$. Furthermore, we perform a Wick rotation to obtain the retarded self-energy. The only term that changes in the self-energy is

$$\frac{1}{-i\hbar\omega_n - \epsilon(\mathbf{p}) + \mu_{\downarrow} + \hbar\omega'} \rightarrow i\pi\delta(\hbar\omega - \epsilon(\mathbf{p}) + \mu_{\downarrow} - \hbar\omega') + \mathcal{P} \left(\frac{1}{\hbar\omega - \epsilon(\mathbf{p}) + \mu_{\downarrow} - \hbar\omega'} \right), \quad (13)$$

with the symbol \mathcal{P} symbolizing the principal value of the fraction. With the help of the relationships above, we find for the imaginary part of the self-energy

$$\begin{aligned}R(\mathbf{k}_+, \omega) &:= -\text{Im}(\hbar\Sigma^{(+)}(\mathbf{k}_+, \omega)) = -\frac{\pi g_{\text{mol}}^2}{V} \sum_{\mathbf{p}} \int_{-\infty}^{\infty} d\hbar\omega' \rho_{\uparrow}(\mathbf{p} + \mathbf{k}_+, \omega') \delta(\hbar\omega - \epsilon(\mathbf{p}) + \mu_{\downarrow} - \hbar\omega') \left(e^{-\beta\hbar\omega'} - e^{-\beta(\epsilon(\mathbf{p}) - \mu_{\downarrow})} \right) \\ &= \frac{\sqrt{\pi} g_{\text{mol}}^2 \beta \exp(\beta\mu_{\downarrow}) (1 - \exp(-\beta\hbar\omega))}{\Lambda^3 \sqrt{2(2\beta\epsilon(\mathbf{k}_+) + (\hbar\beta\Gamma)^2)}} \exp \left(\frac{-\beta(\epsilon(\mathbf{k}_+) + \Delta - \Delta\mu - \hbar\omega)^2}{2((\hbar\beta\Gamma)^2 + 2\beta\epsilon(\mathbf{k}_+))} \right),\end{aligned} \quad (14)$$

with $\mathbf{k}_+ = (0, 0, k_z)$ the wave number for photons in the condensate. By setting $\Delta\mu = 0$ and taking the part of the expression above proportional to N_{\downarrow} , we obtain the absorption cross section at equilibrium. This reduces in the $k_z = 0$ case to

$$\sigma(\omega)|_{k_z=0} = \frac{\sqrt{2\pi} g_{\text{mol}}^2 \exp \left(-\frac{(\hbar\omega - \Delta)^2}{2\hbar^2\Gamma^2} \right)}{\hbar^2\Gamma c_{\text{med}}}. \quad (15)$$

Now we compare the absorption cross section both for $k_z = 0$ and $k_z \neq 0$ to the experimental data for the fluorescent dye [3, 4]. The absorption spectrum for the dye is asymmetric and impossible to fully reproduce within this simple treatment. However, we can perform a fit to the line shape and obtain the coupling constant g_{mol} , the lifetime Γ and detuning Δ . As it turns out the result is almost (or in very good approximation) independent of the exact value k_z , and therefore from now onwards we take $k_z = 0$, thereby simplifying our treatment considerably.

III. BOX-DIAGRAM

We now evaluate the photon-photon interacting strength in the condensate, i.e., with Matsubara frequency zero, and set $k_z = 0$, as is justified by the previous section. Furthermore, by using $G_{\downarrow}^2(\mathbf{p}, m) = -\hbar\partial_{\downarrow}G_{\downarrow}(\mathbf{p}, m)$, we obtain

$$\begin{aligned}\Gamma^{(4)}(\mathbf{0}, \mathbf{0}, \mathbf{0}, 0, 0, 0) &= \frac{g_{\text{mol}}^4}{\hbar^3\beta V} \partial_{\downarrow} \sum_{\mathbf{p}, m} G_{\uparrow}^2(\mathbf{p}, m) G_{\downarrow}(\mathbf{p}, m) \\ &= \frac{g_{\text{mol}}^4 \partial_{\downarrow}}{2\pi\hbar^4\beta\Gamma^2\Lambda^3} \int_{-\infty}^{\infty} d\hbar\omega \int_{-\infty}^{\infty} d\hbar\omega' \exp \left(\beta\mu_{\downarrow} - \frac{1}{2(\hbar\Gamma)^2} \left((\hbar\omega + \Delta\mu - \Delta)^2 + (\hbar\omega' + \Delta\mu - \Delta)^2 \right) \right) \\ &\quad \times \frac{1}{\omega - \omega'} \left(\frac{1}{\omega'} (1 - e^{-\beta\hbar\omega'}) - \frac{1}{\omega} (1 - e^{-\beta\hbar\omega}) \right)\end{aligned} \quad (16)$$

where we again performed the Matsubara summation, we took the limit $N_{\text{FD}}(x) \rightarrow N_{\text{MB}}(x)$ and finally performed the \mathbf{p} -integral. After we have substituted Eq. (12), we perform the differentiation. Setting $\Delta\mu - \Delta := \mu - \delta$ and introducing the dimensionless quantities $\omega := \beta\hbar\omega$, $\omega' := \beta\hbar\omega'$, $\delta := \beta\delta$ and $\mu := \beta\mu$, we obtain

$$\begin{aligned} \Gamma^{(4)}(\mathbf{0}, \mathbf{0}, \mathbf{0}, 0, 0, 0) &= \frac{g_{\text{mol}}^4 \beta n_{\text{mol}}}{2\pi\hbar^2 \Gamma^2 \{1 + \exp(\mu - \delta + (\beta\hbar\Gamma)^2/2)\}} \int_{-\infty}^{\infty} d\omega \int_{-\infty}^{\infty} d\omega' (\omega - \omega')^{-1} \\ &\quad \times \exp\left(-\frac{1}{2(\beta\Gamma\hbar)^2} \left((\omega + \mu - \delta)^2 + (\omega' + \mu - \delta)^2\right)\right) \\ &\quad \times \left(\frac{1}{\omega'}(1 - e^{-\omega'}) - \frac{1}{\omega}(1 - e^{-\omega})\right) \left(1 + \frac{1}{(\beta\hbar\Gamma)^2}(\omega + \omega' + 2\mu - 2\delta)\right) \\ &:= \frac{g_{\text{mol}}^4 \beta n_{\text{mol}}}{\hbar^2 \Gamma^2} f(\mu - \delta), \end{aligned} \tag{17}$$

with $f(\mu - \delta)$ a smooth dimensionless function peaked around zero. As the photon gas is confined to two dimensions we must scale $\Gamma^{(4)} \rightarrow \Gamma^{(4)}/D_0$ to obtain the effective coupling constant g of the photons in the condensate, with D_0 the length scale corresponding to the fixed longitudinal momentum. In general the length scale is given by $D_0 = q\pi/k_z$, with q the number of wavelengths in the standing wave in the longitudinal direction, which is typically 7 or 8 in the experiments of interest to us [5–7].

-
- [1] A.-W. de Leeuw, H.T.C. Stoof and R.A. Duine, Phys. Rev. A **88**, 033829 (2013).
 - [2] H.T.C. Stoof, K.B. Gubbels and D.B.M. Dickerscheid, *Ultracold Quantum Fields*, Springer (2009).
 - [3] R.R. Birge, *Kodak Laser Dyes*, Kodak publication JJ-169.
 - [4] J.R. Lakowicz, *Principles of fluorescence spectroscopy*, Springer (2006).
 - [5] J. Klaers, J. Schmitt, F. Vewinger and M. Weitz, Nature **468**, 545 (2010).
 - [6] J. Klaers, J. Schmitt, T. Damm, F. Vewinger and M. Weitz, Appl. Phys. B **105**, 17 (2011).
 - [7] J. Schmitt, T. Damm, D. Dung, F. Vewinger, J. Klaers and M. Weitz, Phys. Rev. Lett. **112**, 030401 (2014).

